THE ASTROPHYSICAL JOURNAL, 507:327–338, 1998 November 1

ELECTRON ACCELERATION IN SUPERNOVA REMNANTS AND DIFFUSE GAMMA RAYS ABOVE 1 GeV

MARTIN POHL
Danish Space Research Institute, Juliane Maries Vej 30, 2100 Copenhagen Ø, Denmark; mkp@dsri.dk
AND
JOSEPH A. ESPOSITO
NASA Goddard Space Flight Center, Code 662, Greenbelt, MD 20771
Received 1997 October 13; accepted 1998 June 10

ABSTRACT

The recently observed X-ray synchrotron emission from four supernova remnants (SNRs) has strengthened the evidence that cosmic-ray electrons are accelerated in SNRs. We show that if this is indeed the case, the local electron spectrum will be strongly time-dependent, at least above roughly 30 GeV. The time dependence stems from the Poisson fluctuations in the number of SNRs within a certain volume and within a certain time interval. As far as cosmic-ray electrons are concerned, the Galaxy looks like actively bubbling Swiss cheese rather than a steady, homogeneously filled system. Our finding has important consequences for studies of the Galactic diffuse gamma-ray emission, for which a strong excess over model predictions above 1 GeV has recently been reported. While these models relied on an electron injection spectrum with index 2.4 (chosen to fit the local electron flux up to 1 TeV), we show that an electron injection index of around 2.0 would (1) be consistent with the expected Poisson fluctuations in the locally observable electron spectrum and (2) explain the above-mentioned gamma-ray excess above 1 GeV. An electron injection index of around 2 would also correspond to the average radio synchrotron spectrum of individual SNRs. We use a three-dimensional propagation code to calculate the spectra of electrons throughout the Galaxy and show that the longitude and latitude distribution of the leptonic gamma-ray production above 1 GeV is in accord with the respective distributions for the gamma-ray excess. Finally, we point out that our model implies a strong systematic uncertainty in the determination of the spectrum of the extragalactic gamma-ray background.

Subject headings: acceleration of particles — cosmic rays — gamma rays: theory — supernova remnants

1. INTRODUCTION

As was first observed by *OSO 3* (Kraushaar et al. 1972), the dominant feature of the high-energy γ-ray sky is the intense emission from the Galactic plane. Later, the complete *SAS 2* (Fichtel et al. 1975) and *COS B* (Mayer-Hasselwander et al. 1982) data gave evidence for a correlation between the γ-ray emission and the spatial structures of the Galaxy. The intensity distribution and the spectral form of the emission have led to the consensus that the diffuse γ radiation is primarily produced by interactions between Galactic cosmic-ray particles and the interstellar medium, and to a small extent by unresolved Galactic point sources (Bloemen 1989; Strong 1995). The EGRET observations of the Magellanic Clouds have shown that cosmic-ray nucleons in the energy range below 100 GeV are almost certainly Galactic (Sreekumar et al. 1993), while the observations made with the OSSE and COMPTEL instruments aboard *CGRO* have provided strong evidence that cosmic-ray electrons are Galactic (Schlickeiser et al. 1997; see also Fazio, Stecker, & Wright 1966). Thus, the diffuse Galactic γ-ray emission can tell us about the propagation of cosmic rays from their sources to the interaction regions, thus complementing the direct particle measurements by balloon and satellite experiments.

The greater sensitivity and spatial and energy resolution of EGRET compared to *SAS 2* and *COS B* permit a much more detailed analysis of the diffuse Galactic γ-ray emission than was possible with the earlier experiments. The spatial and spectral distribution of the diffuse emission within 10° of the Galactic plane have recently been compared with a model calculation of this emission based on realistic interstellar matter and photon distributions and dynamical balance (Hunter et al. 1997), i.e., on cosmic rays having the same spectrum and composition everywhere in the Galaxy and with an intensity that follows the surface density of thermal gas convolved with a Gaussian with dispersion $\sigma = 1.7$–2.0 kpc (Bertsch et al. 1993). The distribution of the total intensity above 100 MeV agrees surprisingly well with the model predictions. However, at higher energies above 1 GeV, the model systematically underpredicts the γ-ray intensity. If the model is scaled up by a factor of 1.6, the model prediction and the observed intensity above 1 GeV agree well. Thus, the model displays a deficit of $\sim 38\%$ of the total observed emission that depends, if at all, only weakly on location. At energies above 1 GeV, around 90% of the model intensity is due to π^0 decay, i.e., hadronic processes, and only 10% is due to interactions of electrons.

There are a number of possible explanations for this deficit:

1. A miscalibration of EGRET could cause an overestimation of the intensity above 1 GeV. This possibility is highly unlikely. Point sources generally show power-law spectra without spectral hardening above 1 GeV. It would require an extreme level of cosmic conspiracy for a calibration error to mimic a general power-law behavior in the spectra of cosmic γ-ray sources.

2. The kinematics of π^0 production may be poorly understood. Detailed Monte Carlo calculations have shown (Mori 1997) that models based on current knowledge of particle interactions give results for the π^0 spectra that do

not differ much from simple isobar plus scaling descriptions (Dermer 1986). It is unlikely that the cosmic-ray nucleon spectrum in the solar vicinity is softer than that elsewhere in the Galaxy. The local cosmic-ray spectrum samples sources within a few kpc in distance and a few times 10^7 yr in time. Since the observed deficit appears to be independent of Galactic longitude, the sources of cosmic rays within a few kpc from the Sun would have to be different from those in the inner Galaxy and those in the outer Galaxy. We have also tested and verified that the uncertainties in the local interstellar cosmic-ray spectrum below a few GeV are by far not sufficient to account for the deficit. The uncertainties arising from our limited knowledge of the cosmic-ray nucleon spectrum and the nucleon-nucleon interaction kinematics can be estimated to be on the order of a few percent.

3. There may be unresolved point sources that contribute strongly at higher γ-ray energies. The only known class of objects with appropriate spectra are pulsars. Based on the properties of the six identified γ-ray pulsars, it has been found that unresolved pulsars would indeed contribute mainly between 1 and 10 GeV (Pohl et al. 1997b). However, to account for all the deficit it would be necessary for more than 30 pulsars be detectable by EGRET as point sources. This can be compared with less than 10 unidentified γ-ray sources that are not variable (McLaughlin et al. 1996) and show pulsar-like spectra (Merck et al. 1996). In addition, the latitude distribution of the γ-ray emission from unresolved pulsars is inconsistent with that of the observed emission. Unresolved pulsars will contribute 6%–10% of the observed γ-ray intensity above 1 GeV and around 3% in the energy band between 100 MeV and 1 GeV (Pohl et al. 1997b); thus, they can account for only a small fraction of the high-energy γ-ray deficit.

All in all, the effects described above can account only for a small fraction of the deficit, or can add only small systematic uncertainties. In this paper we will investigate whether the remaining deficit of 30%–35% may be caused by inverse Compton emission of high-energy electrons. Leptonic processes contribute only around 10% of the intensity above 1 GeV in the model of Hunter et al. (1997), which corresponds to $\sim 6\%$ of the total observed intensity. Thus, the leptonic contribution would have to be increased to 35%–40% of the total observed emission to explain all the deficit.

The Galactic distribution of cosmic-ray electrons is intimately linked to the distribution of their sources. The recently discovered evidence of X-ray synchrotron radiation from the four supernova remnants SN 1006 (Koyama et al. 1995), RX J1713.7−3946 (Koyama et al. 1997), IC 443 (Keohane et al. 1997), and Cas A (Allen et al. 1997) supports the hypothesis that Galactic cosmic-ray electrons are accelerated predominantly in SNRs. X-ray synchrotron radiation implies TeV γ-ray emission from the Comptonization of the microwave background at a flux level that depends only on the average magnetic field strength (Pohl 1996), and indeed the detection of the remnant SN 1006 at TeV energies has recently been announced (Tanimori et al. 1997). Interestingly, there is no clear observational proof that the nuclear component of cosmic rays is likewise accelerated in SNRs. The acceleration of cosmic-ray nucleons in SNRs should lead to observable flux levels at TeV energies (Drury, Aharonian, & Völk 1994), but with a spectrum different from that of the leptonic emission. The generally tight upper limits for TeV emission from the nearest SNR (Lessard et al. 1995; Buckley et al. 1998) are in conflict with simple shock-acceleration models for cosmic-ray nucleons in SNRs.

Most of the radio synchrotron spectra of SNRs can be well represented by power laws with indexes around $\alpha \simeq 0.5$, corresponding to electron injection indexes of $s \simeq 2.0$ (Green 1995). This is in accord with predictions based on models of particle acceleration (Blandford & Eichler 1987). However, it differs from the electron injection spectral index of $s = 2.4$ that has been inferred from the locally observed electron spectrum (Skibo 1993) and that has subsequently been used in the model of Galactic γ-ray emission by Hunter et al. (1997). The contribution of cosmic-ray electrons to the Galactic γ-ray spectrum at high energies depends strongly on their injection spectral index. If the acceleration cutoff energy is high enough, the leptonic γ-ray emission may even dominate at TeV–PeV energies (Porter & Protheroe 1997). A change in the electron injection index by $\delta s = 0.4$ could increase the inverse Compton emissivities at a few GeV by an order of magnitude or more.

Let us suppose that for some reason the local cosmic-ray electron spectrum is different from the average electron spectrum in the Galaxy. Then the following scenario appears viable: the bulk of cosmic-ray electrons are accelerated in SNRs with an injection index around $s \simeq 2.0$. The leptonic γ-ray emission at a few GeV would be much stronger than in the Hunter et al. (1997) model, and it may explain a substantial fraction of the discrepancy between their model and the observed spectra. Therefore, if we find a mechanism or an effect that would cause the local electron spectrum to be different from the Galactic average, we may in a second step reassess the γ-ray spectra produced by Galactic cosmic rays without having to assume an electron injection index of $s = 2.4$.

It has been noted before that the spatial distribution of cosmic-ray sources affects the locally observable spectra (Cowsik & Lee 1979; Lerche & Schlickeiser 1982a). As far as electron acceleration in SNRs is concerned, there is no evidence that the star formation activity and thus the SNR production rate in the solar vicinity is significantly less than the Galactic average. In the next section we will show that for cosmic-ray electrons, unlike nucleons, the local spectra above a certain energy can deviate from the Galactic average, even if the spatial distribution of cosmic-ray-accelerating SNRs is homogeneous. This is a result of the discrete nature of SNRs in both space and time. We will use this finding in § 3 to model the high-energy γ-ray excess as result of inverse Compton emission of cosmic-ray electrons, albeit with a harder injection spectrum than conventionally assumed.

2. THE TIME DEPENDENCE OF THE LOCAL ELECTRON SPECTRUM

The spectrum of cosmic-ray electrons has been discussed before (Cowsik & Lee 1979) with regard to the contribution of discrete sources such as SNRs. These authors have investigated the case of continuously active sources and have concluded that it requires sources situated within a few hundred parsecs of the solar system, in order for the energy losses of electrons not to induce a cutoff in the energy spectrum. Since the required number of active sources exceeds the number of supernova remnants by an order of magnitude, SNRs were found unlikely to be the only source of cosmic-ray electrons between 1 GeV and 1 TeV. In that

paper, the diffusion coefficient had been assumed independent of energy. With the usual energy dependence $D \propto E^{(0.3-0.6)}$, some of the statements of Cowsik & Lee (1979) would have to be relaxed.

In this section we will consider the finite lifetime of SNRs or other possible cosmic-ray accelerators, together with the random distribution of SNRs in space and time. The latter induces a time dependence in the local electron spectrum at higher energies that stems from the Poisson fluctuations in the number of SNRs within a certain distance and time interval. As we will see, the discreteness of sources does not simply cause a cutoff in the electron spectrum, but makes it variable with time and thus unpredictable beyond a certain energy.

Since effects of the discreteness of sources show up only at higher particle energies, we can describe the propagation of cosmic-ray electrons at energies of 1 GeV to 1 TeV by a simplified transport equation,

$$\frac{\partial N}{\partial t} - \frac{\partial}{\partial E}(bE^2 N) - DE^a \nabla^2 N = Q\,, \tag{1}$$

where we consider continuous energy losses by synchrotron radiation and inverse Compton scattering, an energy-dependent diffusion coefficient DE^a, and a source term Q. The Green's function for this problem can be found in the literature (Ginzburg & Syrovatskii 1964):

$$G(r, r', t, t', E, E') = \frac{\delta[t - t' + (E - E')/bEE']}{bE^2[4\pi\lambda(E, E')]^{3/2}} \times \exp\left[-\frac{(r - r')^2}{4\lambda(E, E')}\right], \tag{2}$$

where

$$\lambda(E, E') = \frac{D}{b(1 - a)}(E^{a-1} - E'^{a-1})\,. \tag{3}$$

In the case of discrete sources, the injection term Q is a sum over all the sources. For an individual source showing up at time t_0 and injecting for a time period τ, we can write

$$Q_i = q_0 E'^{-s}\delta(r')\Theta(t' - t_0)\Theta(t_0 + \tau - t')\,. \tag{4}$$

Without loss of generality, we can set $t = 0$ and obtain

$$N = q_0 E^{-s} \int_{-1/bE}^{0} \times dt' \frac{\Theta(t' - t_0)\Theta(t_0 + \tau - t')\exp(-r^2/4\Lambda)}{(4\pi\Lambda)^{3/2}(1 + bEt')^{2-s}}\,, \tag{5}$$

where

$$\Lambda = \frac{DE^{a-1}}{b(1 - a)}[1 - (1 + bEt')^{1-a}] \tag{6}$$

and r is the distance between source and observer. N gives the contribution to the local electron spectrum provided by a single source (SNR) at distance r, that is (or was) injecting electrons for a time period τ, starting at t_0. The local spectrum of electrons can now be obtained by summing the contributions from all individual sources. In our case, for ease of exposition and computation the distribution of SNRs is assumed to be a homogeneous disk of radius $r_s = 15$ kpc and half-thickness $z_s = 0.14$ kpc. Other choices for the spatial distribution of SNRs do not impose serious changes in the results, as long as the distribution is not structured on subkiloparsec scales.

The numerical procedure is as follows. For each volume element δV, the expected number of SNRs injecting cosmic rays within the time interval δt is given by

$$N_\lambda = \frac{\delta V\,\delta t}{V_{\rm tot}\,t_{\rm inj}}\,, \tag{7}$$

where $V_{\rm tot}$ is the total volume of the source distribution and $t_{\rm inj} = 55$ yr is the inverse of the supernova rate (Cappelaro et al. 1997). The term δt has to be the maximum look-back time in our model, the sum of the SNR lifetime τ and the electron energy loss time $t_l = 1/b(1\ \text{GeV})$ at 1 GeV, the lowest energy considered here. At any given time, the actual number of SNRs in that volume element is a Poissonian random number with mean N_λ, and each of the SNRs has a birth date that is a random number uniformly distributed within $[-\tau, -t_l, 0]$. The final electron spectrum is then derived by summing over the contributions of the individual SNRs per volume element and summing over all relevant volume elements. We calculate 400 such random spectra, and thus derive the distribution of possible spectra and their spread.

In Figure 1 we show the resulting range of local electron spectra compared with the observed spectra (Ferrando et al. 1996; Golden et al. 1994, 1984; Tang 1984; Taira et al. 1993). The energy density of the ambient photon fields plus that of the perpendicular component of the magnetic field strength is in total taken to be 3.5 eV cm^{-3}. The changes in the Compton cross section in the Klein-Nishima regime of optical and near-infrared photon fields are neglected. The diffusion coefficient is $D = 4 \times 10^{27}$ cm^2 s^{-1} at 1 GeV and increases with energy to the power $a = 0.6$, in accord with results for a two-dimensional diffusion model fitted to the local spectra of 13 primary and secondary cosmic-ray nuclei at rigidities between 1 and 10^3 GV (Webber, Lee, & Gupta 1992). At these energies, electrons and nuclei will scatter off the same turbulence, except for the helicity, and thus their diffusion behavior is expected to be similar. The injection spectral index of electrons is $s = 2.0$, which corresponds to the mean synchrotron spectral index of individual SNRs (Green 1995).

The solar modulation of electrons at energies of a few GeV has a strong effect on the observed spectrum. Note the difference between the spectrum observed when the modulation level was high (Golden et al. 1994) and the spectrum observed during the passage of *Ulysses* over the solar south pole (Ferrando et al. 1996). We have crudely approximated the effect of solar modulation using the force-field approach (Gleeson & Axford 1968), with $\Phi = 400$ MV. Thus, we probably overestimate the modulation in case of the *Ulysses* data and underestimate it for the Golden et al. (1994) data.

The spectra at a given time are not necessarily smooth. There is no preference for the usual broken power laws or power laws with exponential cutoffs. In fact, the individual spectra are bumpy above ~ 50 GeV, and some display step-like features. As an example, we show a particular spectrum by the dash-dotted line in Figure 1; it is slightly on the low side between 10 and 100 GeV, where it suffers further softening, before it abruptly hardens at 300 GeV.

Below 10 GeV, the local electron spectrum is well determined. Between 10 and 100 GeV, it varies with time by a

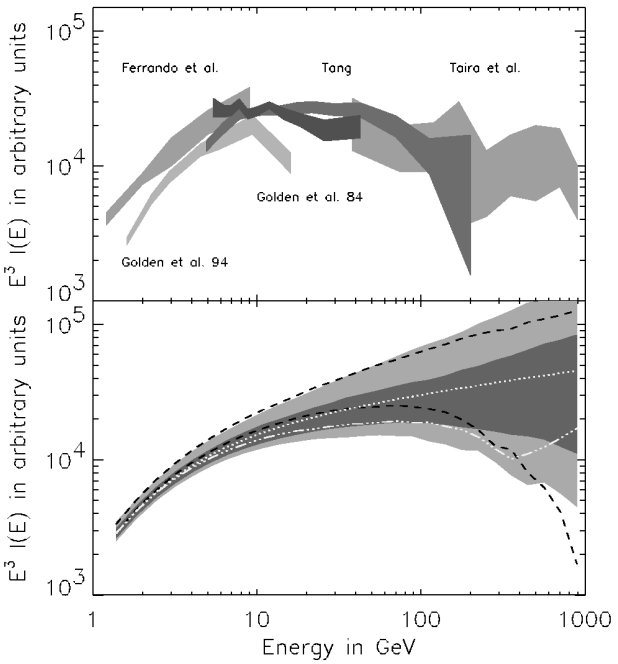

FIG. 1.—Locally observed electron spectra (*top panel*) compared with the range of possible spectra in our model (*bottom panel*). The parameters of the model are given in the main text. For each experiment, the 1 σ uncertainty range is indicated by a gray-shaded band connecting the data points at the mean energies of the corresponding energy bins. The scatter between the results of different experiments indicates the level of systematic uncertainties. The range of possible spectra in our model is given by the gray-shaded bands in the lower panel. For 68% of the time the locally observed spectra will be in the dark gray shaded region, and 95% of the time they will be within the light gray shaded region. The black dashed line shows the 68% range for a weaker energy dependence of the diffusion coefficient ($a = 0.33$ instead of $a = 0.6$) to show the influence of this parameter. The white dash-dotted line shows one of the 400 random spectra as a particular example of what may be observed. The white dotted line indicates the time-averaged spectrum. The effect of solar modulation is taken into account for all model spectra using a force-field parameter $\Phi = 400$ MV (Gleeson & Axford 1968). The data are not in conflict with the range of possible spectra in our model.

factor of 2 or 3, and above 100 GeV it is completely unpredictable. Changes in the absolute numbers for the diffusion coefficient and the radiative energy losses do not change the basic behavior, but they can shift the transition between weak and strong variability to lower or higher energies. If the energy dependence of the diffusion coefficient is weaker, i.e., $a < 0.6$, the transition between weak and strong variability will be faster, and vice versa (a slower transition for higher powers than $a = 0.6$). For comparison, we have indicated the result for an energy dependence of the diffusion coefficient, $D \propto E^{0.33}$.

As shown in Figure 1, the high-energy data for the local electron flux are in accord with an injection spectral index of $s = 2.0$, although in a model with steady injection and a smooth source distribution these data would require an injection index of around 2.4 (Skibo 1993). Concerning the distribution of high-energy electrons, the Galaxy would look like Swiss cheese, with holes and regions of higher density. In the line-of-sight integrals, which are relevant for comparison with the EGRET γ-ray data, averaging over holes and high-density regions will give the same result as a model with steady injection, but with a source index of 2.0 instead of 2.4. At higher latitudes, the line of sight will be so short that regions of low or high electron density will be resolved. The leptonic γ-ray spectra in the direction of the Galactic poles should be relatively soft, since the line-of-sight integral of the γ-ray emissivity will be dominated by the soft local spectrum.

The absolute electron flux is reproduced if each SNR provides an energy input of 10^{48} ergs in the form of electrons, which is 1/1000 of the canonical value of 10^{51} ergs for the kinetic energy input per supernova. Taken over a lifetime of 10^5 yr, the corresponding power of 5×10^{35} ergs s^{-1} is less than the X-ray luminosity of SN 1006 alone.

The time variability of the high-energy cosmic-ray spectrum will not be related to or even be synchronous with the variability in the flux of low-energy cosmic-ray nucleons, which can be traced by cosmogenic unstable isotopes in sediments (Sonnett et al. 1987; McHargue, Damon, & Donahue 1995; Kocharov 1996) or meteorites (Bonino 1996).

A few notes should be added. We have taken supernova explosions to be completely independent of each other. One might expect some level of correlation in OB associations and supernova remnants in OB associations (SNOBs), which would make the basic effect of time dependence even more dramatic, since the OB associations and SNOBs would act as single sources, with longer lifetimes but much smaller frequencies of occurrence.

Another important point is that we have assumed that all electron sources produce the same spectrum. In reality this need not be the case. Some SNRs will produce electrons with harder spectra, and another group of SNRs will provide softer spectra. It may be that the spectral form depends on the age of the SNR. In fact, the radio data show that SNRs do have different synchrotron spectra (Green 1995). If we take the electron injection spectral index of an individual SNR not as a fixed number but as a random variable following some probability function, the time-averaged spectrum (Fig. 1, *dotted line*) will produce a positive curvature. The level of time variability, on the other hand, will increase. The dark and light shaded regions in the lower panel of Figure 1, in which the spectrum is contained for 68% and 95% of the time, respectively, extend beyond those for the fixed injection index.

A final note concerns secondary positrons and electrons. These particles are generated subsequent to interactions of cosmic-ray nucleons with ambient gas, so the effect discussed here does not apply and the local spectrum of secondary electrons will not vary. Thus, the observed positron fraction will also exhibit variability anticorrelated with that of the primary electron spectrum. If we are indeed living in a hole in the distribution of high-energy electrons, then the positron fraction above, say, 20 GeV will be above the level expected in steady injection models, if the gas density within ~ 1 kpc from the Sun is not also subaverage. This might explain the observed positron fraction in that energy range, which is indeed slightly above the model predictions (Barwick et al. 1997).

We have seen that the discreteness of sources of cosmic-ray electrons causes a strong variability in the local electron spectrum at higher energies. Therefore, the high-energy electron spectrum does not prescribe our choice of electron injection spectrum in propagation models.

If we consider γ-ray emission in the Galactic plane, the line-of-sight integral of the emissivity will correspond to an averaging over the different variability states, and hence the

γ-ray intensity calculated with time-dependent models will not differ significantly from the results of steady-state models. The latter are much easier to compute and thus preferable, but they will in general not be able to reproduce the local high-energy electron spectrum correctly. On the other hand, in the absence of reliable data on the position and age of all nearby SNRs, it is also impossible to calculate the time-dependent local electron spectrum precisely, so we can only infer the level of variability. Therefore, we feel that if the acceleration of electrons occurs predominantly in SNRs, the γ-ray emission in the Galactic plane can be sufficiently well described with steady-state models, provided that the model is not required to fit the local electron data above ~ 30 GeV. In the next section we will discuss a steady-state model for the diffuse leptonic γ-ray emission for an injection index of 2.0.

3. THE PROPAGATION OF ELECTRONS IN THE STEADY-STATE CASE

There is a wealth of literature on the topic of electron propagation in the Galaxy, including analytical solutions for the one- and two-dimensional diffusion and diffusion-convection problems (Ginzburg & Syrovatskii 1964; Berkey & Shen 1969; Lerche & Schlickeiser 1981, 1982b; Pohl & Schlickeiser 1990). These solutions can be well described in their basic behavior by the concept of the catchment sphere (Webster 1970). The energy losses prevent electron propagation farther from their source than a critical distance ρ, defined by an equality of the timescales for transport and energy loss, so that the spatial dependence of the Green's function of the problem is basically a function that is a constant for distances of less than ρ and zero beyond ρ. If the transport is governed by diffusion, and if the energy loss terms do not strongly depend on location, then ρ will not strongly depend on direction, and thus a source of cosmic rays at the position (x', y', z') would fill a sphere of radius ρ with cosmic rays. Therefore, we can separate the spatial problem and the energy problem, and approximate the solution to the spatial problem by a Gaussian function for the catchment sphere. The Gaussian function is exact at higher energies, where radiative energy losses dominate, but is a crude approximation at very low energies, where ionization and Coulomb losses are important.

We will include escape as a catastrophic loss term, which limits ρ to some maximum value. This approximates the effect of a sudden increase of the diffusion coefficient at a certain height above the Galactic plane (Lerche & Schlickeiser 1982b). We regard this as a better description than a finite boundary with density and density gradient set to zero at $L_{\rm halo}$ a few kpc above the Galactic plane, since for a physical escape solution the density outside the diffusion region relates to that inside as

$$n_{\rm out} \simeq \frac{n_{\rm in} L_{\rm halo}}{\tau_{\rm esc} \beta c} \simeq 10^{-4} n_{\rm in} \left(\frac{E}{\rm GeV} \right)^{0.6} , \tag{8}$$

and thus is definitely not zero. With a diffusion coefficient $D = D_0 E^a$, E being the kinetic energy, we have

$$\rho(E) = \sqrt{4 D_0 E^a} \sqrt{\tau_{\rm eff}} , \tag{9}$$

where

$$\tau_{\rm eff}^{-1} = \tau_{\rm esc}^{-1} + \tau_{\rm loss}^{-1} . \tag{10}$$

We can write the differential number density of cosmic rays at position (x, y, z) coming from a source at (x', y', z') as

$$\delta N = \frac{1}{(\sqrt{\pi}\rho)^3 |\dot{E}|} \times \int_E du\, Q(u) \exp \left[- \int_E^u \frac{dv}{\tau_{\rm esc}(v) |\dot{E}(v)|} \right] \exp \left(- \frac{r^2}{\rho^2} \right) , \tag{11}$$

where

$$r^2 = (x - x')^2 + (y - y')^2 + (z - z')^2 , \tag{12}$$

$\dot{E}$ is the energy loss term, and $Q(E)$ is the source spectrum at position (x', y', z'). Physically, δN is a propagator, and it can be treated as a Green's function. Given the spatial distribution of sources $q(x', y', z')$, we obtain the cosmic-ray spectrum at any position (x, y, z) as

$$N(E) = \int dx'\, dy'\, dz'\, \delta N q(x', y', z') . \tag{13}$$

Our method thus enables us to calculate the three-dimensional distribution of electrons resulting from an arbitrary three-dimensional distribution of sources.

Individual SNRs may accelerate electrons with slightly different spectra. This would result in a positive curvature of the composite injection spectrum (Brecher & Burbidge 1972). To demonstrate the effect of a possible dispersion of the injection spectral index in the electron sources, we assume that the injection indexes for individual SNRs follow a normal distribution,

$$P(s) = \frac{1}{\sqrt{2\pi}\,\mu_s} \exp \left[- \frac{(s - s_0)^2}{2\mu_s^2} \right] , \tag{14}$$

at the energy E_0. Radio spectral index measurements at a few GHz, corresponding to $E_0 \simeq 5$ GeV, indicate $\mu_s \lesssim 0.2$ (Green 1995). Then the source spectrum of primary electrons is given by

$$Q_e = q_e (m_e c^2)^{s-1} E^{-s} \left(\frac{E}{E_0} \right)^{0.5 \mu_s^2 \ln - E/E_0} . \tag{15}$$

For $\mu_s = 0$, this reduces to the conventionally assumed single power law.

The energy losses due to ionization and Coulomb interactions, bremsstrahlung and adiabatic cooling, and synchrotron and inverse Compton emission are well described by

$$-\dot{E} = 7.2 \times 10^{-13} n_{\rm H} \tau \times \left[1 + \frac{\eta}{\tau} \frac{E}{714\, m_e c^2} + \frac{\epsilon U_{\rm mag}}{n_{\rm H} \tau} \left(\frac{E}{3727 m_e c^2} \right)^2 \right] , \tag{16}$$

where we have used the following abbreviations:

$$\epsilon = 0.75 + \frac{U_{\rm rad}}{U_{\rm mag}} ,$$

$$\eta = 1 + n_{\rm H}^{-1} \left(\frac{\rm div\, \boldsymbol{v}}{3 \times 10^{-15}\ {\rm s}^{-1}} \right) + 0.95 \frac{n_e}{n_{\rm H}} ,$$

$$\tau = 1 + 1.54 \frac{n_e}{n_{\rm H}} , \tag{17}$$

where n_H is the neutral gas density, n_e is the density of ionized gas, v is the bulk velocity of electrons, and U is the energy density of the magnetic field and the ambient radiation field in eV cm^{-3}.

We assume the magnetic field strength to be constant over the total volume of the Galaxy, with $B = 10\ \mu$G. As we shall see later, this value leads to synchrotron emission consistent with observations. The interstellar radiation field can be calculated from the respective emissivities for optical and infrared emission, and from the microwave background emission (see Youssefi & Strong 1991 and recent updates by A. W. Strong 1997, private communication). The distribution of ionized gas has been modeled on the basis of pulsar data (Taylor & Cordes 1993). The derivation of the distribution of neutral matter will be discussed below. For the propagation calculation, all parameters of the interstellar medium are averaged over a scale of 1 kpc to mimic the average environmental conditions of a cosmic-ray electron during its life time. A Galactic wind is assumed to operate in the Galactic halo, such that adiabatic cooling outside the disk provides energy losses similar to those from bremsstrahlung inside the disk, i.e., the energy-loss terms can be written independently of the spatial location within a catchment sphere. Note that the energy-loss terms for neighboring catchment spheres may be different, since they are averages over different volumes. The radial extent of the Galaxy is taken to be 16.5 kpc. Note that the computer time consumption scales as the radial extent squared. The calculation of the bremsstrahlung and inverse Compton emissivities is described elsewhere (Pohl 1994).

The energy-loss timescale, which determines the radius of the catchment sphere ρ, can be understood as an ensemble average,

$$\bar{\tau} = \frac{\int_E^\infty dE' Q(E') \int_{E'}^E du \dot{u}^{-1}}{\int_E^\infty dE' Q(E')}, \tag{18}$$

where $Q(E)$ is the electron injection spectrum. This average age can be approximated by

$$\tau_{\rm loss} = \int_{E_c}^E du \dot{u}^{-1}, \quad E_c = 2.718E \tag{19}$$

to better than 30% accuracy, except for the lowest energies. For $E_c \le 714 \tau \eta^{-1} m_e c^2$, corresponding to $E \lesssim 100$ MeV, the average age $\bar{\tau}$ is larger than the e-folding energy-loss timescale. Here the energy losses will also depend explicitly on ρ, since ioniziation and Coulomb interactions occur only in the gas disk. For ease of computation, we will assume $\tau_{\rm loss}$ to be constant at these low energies, as if ionization and Coulomb interactions did not occur. This means that we overestimate ρ but underestimate $\dot{E}$. The two effects work in opposite directions, but may not balance each other. We need to keep in mind that we are using a crude approximation at low electron energies, which for this paper will have an impact only on the bremsstrahlung spectra at $\lesssim 50$ MeV.

We neglect secondary electrons in our model. The locally observed fraction of secondary electrons is on the order of 10% (Barwick et al. 1997), but the fraction may be strongly dependent on position and on the propagation behavior of particles (Schlickeiser 1982). There are basically two arguments that allow us to neglect the secondaries. First, because of the energy dependence of the cosmic-ray secondary-to-primary ratios, secondary electrons will have a production spectrum that is softer than the production spectrum of cosmic-ray nucleons by $\delta s \simeq 0.6$, at least above 1 GeV electron energy. Thus, secondary electrons will have a softer spectrum than primary electrons, so that their contribution to the diffuse Galactic γ-ray emission cannot lead to a hardening of the spectrum, irrespective of the flux. The second argument concerns the luminosity. Since the production cross sections for charged and neutral pions are of the same order, and the electrons take only about two-thirds of the pion energy, the source power supplied to secondary electrons is linked to the hadronic γ-ray luminosity. Only a fraction of the source power is channeled back into γ-ray emission, since synchrotron radiation takes away some energy. Because of the kinematical low-energy cutoff at ~ 100 MeV in the secondary production spectrum and the decrease of hadronic γ-ray luminosity at energies above 1 GeV, the secondary contribution to leptonic γ-ray emission above 100 MeV will always be limited to less than 10% of the γ-ray luminosity arising from π^0-decay (Pohl 1994), and thus will be negligible in this energy range.

3.1. *The Distribution of Gas*

The three-dimensional distribution of thermal material in the Galaxy has been determined by deconvolution of H I surveys for atomic gas and CO surveys for molecular gas with the rotation curve of Clemens (1985). The H I surveys include the Leiden-Greenbank survey (Burton & Liszt 1983; Burton 1985), the Weaver-Williams survey (Weaver & Williams 1973), the Maryland-Parkes survey (Kerr et al. 1986), the high-latitude Parkes survey (Cleary, Heiles, & Haslam 1979), and the Heiles-Habing survey (Heiles & Habing 1974). The CO data are taken from the Columbia survey (Dame et al. 1987), as updated by S. W. Digel & T. M. Dame (1997, private communication). All these data are publicly available from either the Astrophysics Data Catalogues (ADC) or the Centre de Données astronimiques de Strasbourg (CDS) databases. It should be noted that none of these surveys are corrected for stray light. The level of uncertainty in the rotation curve, the position of the Sun, and the noncircular motions of the gas is high, so that our deconvolution should be taken as a model rather than as fact.

The general procedure in the deconvolution process is as follows. The rotation curve is used to calculate the relation between distance and line-of-sight velocity, which is then transformed into a probability distribution for distance on the basis of the actual velocity resolution of the surveys and a turbulent velocity dispersion of 10 km s^{-1} for CO and 25 km s^{-1} for H I. This approach tends to smear out the gas distribution along the line of sight, but relaxes most of the forbidden velocity problem. The near-far ambiguity toward the inner galaxy is resolved by dividing the intensity according to the amplitudes of Gaussian probability functions for the distribution of gas normal to the Galactic plane. These Gaussian probability functions are convolutions of the local gas distribution functions and the spatial resolution function of the particular survey. The effective scale heights of gas on the far side of the Galaxy are thus systematically larger than the local values. As a result, the gas tends to be more evenly distributed over the Galaxy than in other derivations (Hunter et al. 1997), and the deconvolved gas distribution on the far side of the Galaxy will be slightly smeared out normal to the Galactic plane. This has no impact on the calculation of the γ-ray emission, since the column density of gas is always preserved, and it has also no

impact on the cosmic-ray propagation, since our algorithm is based on the gas surface density, which is also preserved.

The H I data are scaled under the assumption of a constant spin temperature of $T_s = 125$ K. The obvious absorption features in the direction of the Galactic center have been replaced by a linear interpolation between the neighboring velocity bins. The distribution of H I normal to the Galactic plane is assumed to be a Gaussian of dispersion $z_c = 0.12 + 0.023(r - 9.5)\Theta(r - 9.5)$ kpc, where r is the Galactocentric radius and Θ is a Heavyside function, with an offset according to the warping of the H I disk (Burton 1976).

The CO data are scaled with an X-factor of 1.25, which is the mean of the best-fit values in published papers on EGRET data analysis (Hunter et al. 1994, 1997; Digel et al. 1995, 1996; Strong & Mattox 1996). In the inner kiloparsec of the Galaxy, the X-factor is reduced to 25% of its nominal value to account for the higher excitation temperature and different metallicity (Sodroski et al. 1995; Arimoto, Sofue, & Tsujimoto 1996). The noise in the CO spectra is preserved in the deconvolution process in order to keep the line-of-sight integral of the density unchanged. The vertical CO distribution is assumed to be a Gaussian of dispersion $z_c = 0.074 + 0.03(r - 9.5)\Theta(r - 9.5)$ kpc, where r is the Galactocentric radius and Θ is a Heavyside function (Dame et al. 1987). The position of the Sun is assumed to be 8.5 kpc from the Galactic center and 15 pc above the plane (Hammersley et al. 1995).

For a region of $\sim 20°$ toward the Galactic center and toward the anticenter, the kinematical resolution is insufficient, and the data have been edited by hand. The distribution of gas in these two regions is basically an interpolation between the results for the adjacent regions. In the anticenter region, any excess over this interpolation has been evenly distributed over all distances, while in the Galactic center region any excess is attributed to the Galactic center. The distribution of gas in the Galactic plane is shown in Figure 2.

3.2. *The Spatial Distribution of Sources*

The true distribution of SNRs in the Galaxy is not well known, as a result of selection effects and the absence of a proper distance measure to the remnants. In many papers (Stecker & Jones 1977; Dogiel & Uryson 1988; Bloemen et al. 1993), the cosmic-ray distribution in the Galaxy has been estimated on the basis of a functional form for the SNR distribution that fits the data for 116 remnants (Kodaira 1974). One of the general findings of these studies is that the overall cosmic-ray distribution is too steep to explain the gradual slope of the γ-ray emissivity over the Galactic

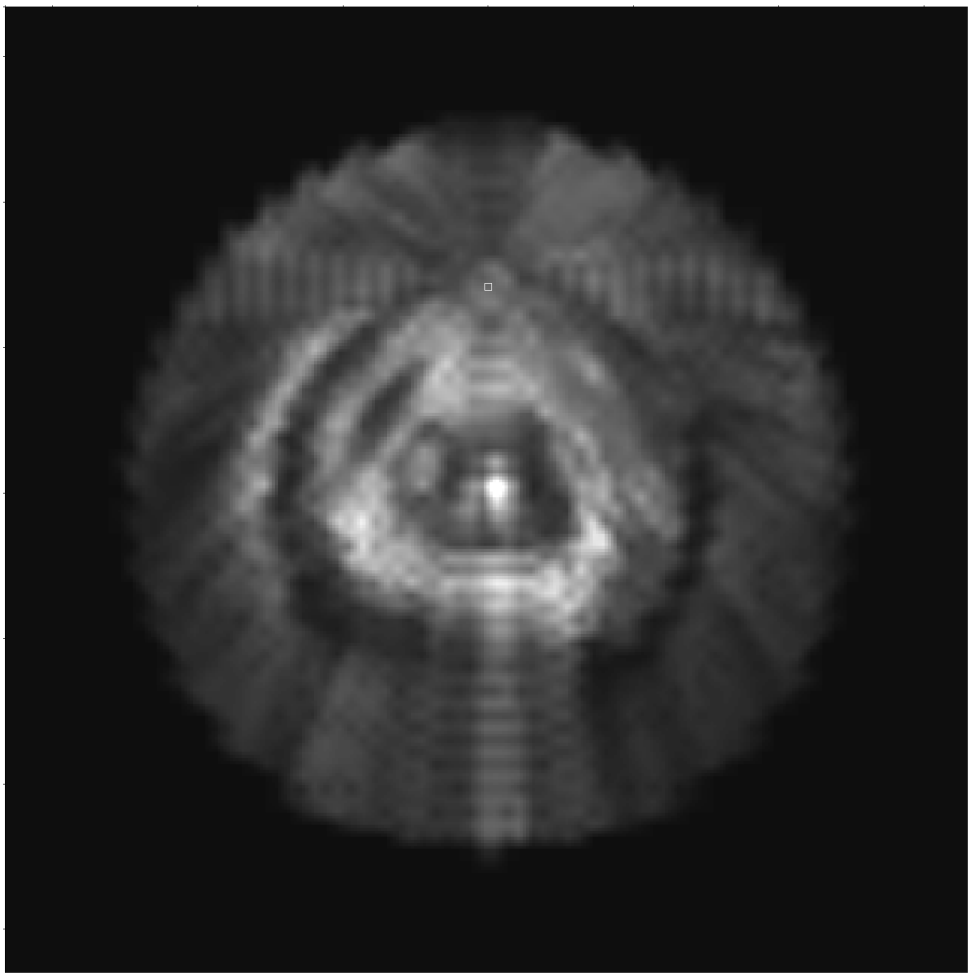

FIG. 2.—Face-on view of the surface density of gas in the Galaxy. The square indicates the position of the Sun. The color scale is linear between surface mass densities of $-2\ M_\odot\ \mathrm{pc}^{-2}$ and $30\ M_\odot\ \mathrm{pc}^{-2}$. The plot includes atomic, molecular, and ionized gas integrated from -500 pc to 500 pc height above the plane.

radius (Strong et al. 1988; Strong & Mattox 1996).

Here we use a revised functional form for the SNR distribution (Case & Bhattacharya 1996) that fits the data for 194 remnants;

$$f(r) = \left(\frac{r}{r_\odot}\right)^{1.69 \pm 0.22} \exp\left[-(3.33 \pm 0.37)\,\frac{r - r_\odot}{r_\odot}\right], \quad (20)$$

where $r_\odot = 8.5$ kpc denotes the distance between the Sun and the Galactic Center. The vertical distribution of SNRs is taken to be box-shaped, with a half-thickness of 150 pc.

Our model allows us to use true three-dimensional source distributions. We know that the Galaxy has structure in the form of spiral arms, a bulge, and so forth. We have thus folded a spiral-arm model (Georgelin & Georgelin 1976; Vallée 1995) with the radial SNR distribution as described above in order to investigate the influence of spiral-arm structure. In the Georgelin & Georgelin (1976) model, the Galaxy has four symmetric arms with pitch angles of around 12°. We have rescaled their model to $r_\odot = 8.5$ kpc. Each spiral arm is described by a Gaussian of dispersion 500 pc, i.e., a FWHM of 1177 pc. The spiral-arm model is normalized in azimuth, so that the integral $\int_0^{2\pi} r\,d\phi$ of that model yields unity, and then folded with the radial SNR distribution. The normalization is required to preserve the radial distribution of SNRs. A face-on view of the resulting source distribution is shown in Figure 3.

4. RESULTS

In this section we show results for two choices of the spatial distribution of sources, a pure SNR distribution and a SNR distribution folded with a model of the spiral arms in the Galaxy. We will also show results for two choices of the injection index: a fixed index $s = 2.0$ for all sources and a normal distribution of indexes with mean 2.0 and dispersion 0.2. We will not vary any other parameter in the propagation model, and we stick to the best-fit values given by Webber et al. (1992). In a forthcoming paper we will extend our model to nucleons and self-consistently determine the propagation parameters that fit the γ-ray data and the local spectra of primary and secondary cosmic rays. In this paper our aim is simply to show that an injection index of around $s = 2.0$ for cosmic-ray electrons is sufficient to explain the observed spectrum of diffuse high-energy γ rays, while leaving all other parameters unchanged.

4.1. *The Local Electron Spectra*

We have shown in § 2 that if electrons are accelerated in SNRs, their local spectra above ~ 30 GeV will strongly depend on time, so that direct electron measurements above this energy may deviate from the average electron spectrum. As a result, we are not required to choose the electron injection index according to the directly observed electron spectrum above ~ 30 GeV. Below a few GeV, on the other

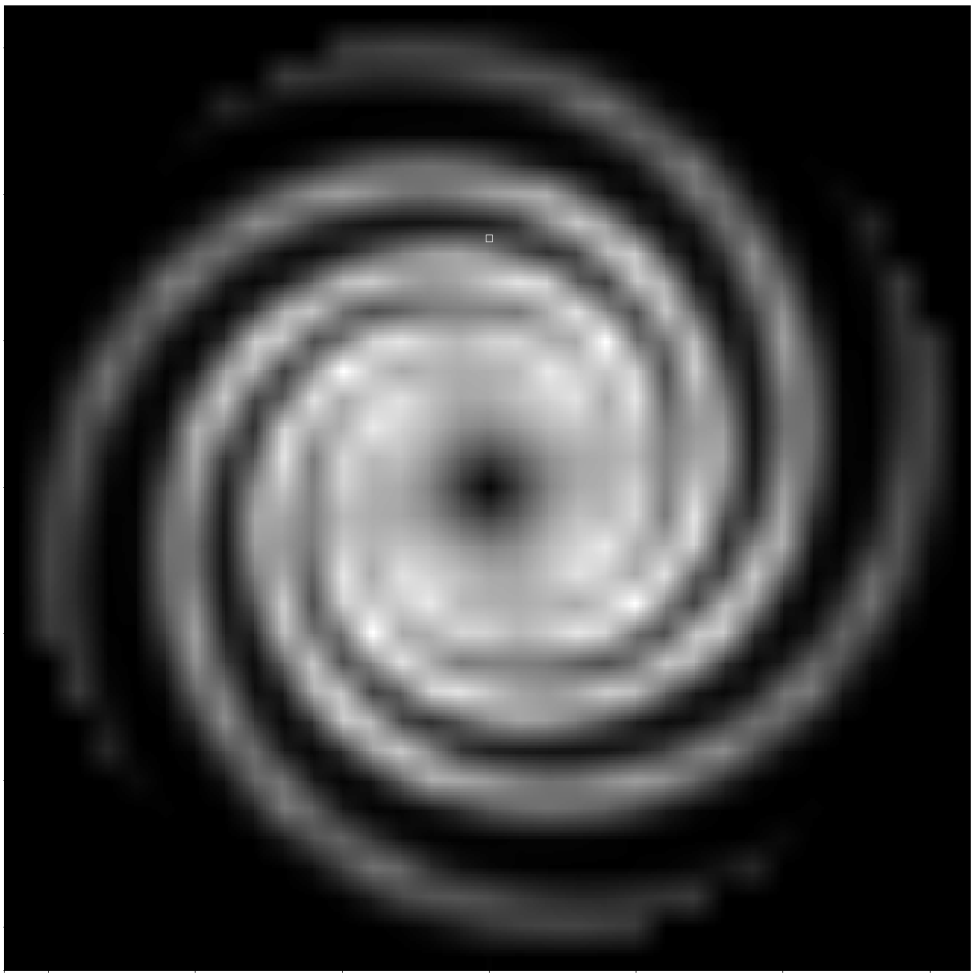

FIG. 3.—Face-on view of the SNR distribution in the Galaxy according to the spiral-arm model. The square indicates the position of the Sun. The color scale is linear between zero and peak value. Note that the Sun is located in an interarm region.

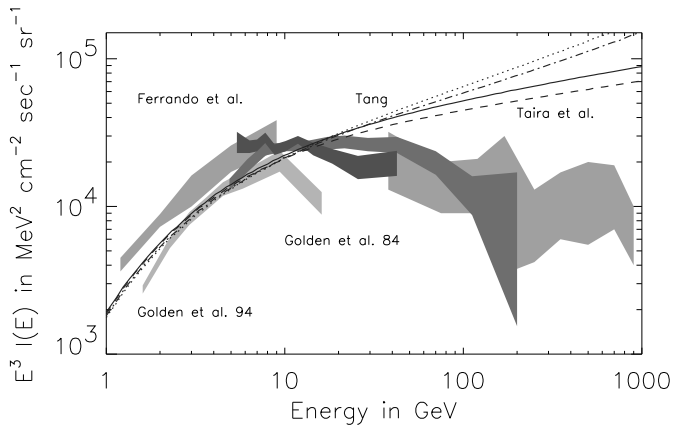

FIG. 4.—Data for the local flux of cosmic-ray electrons compared with the steady-state model spectrum. Solar modulation is taken into account using a force-field parameter $\Phi = 400$ MV (Gleeson & Axford 1968). For the case of pure SNR distribution as electron-source distribution, the solid line shows sources with fixed injection index $s = 2.0$, while the dotted line shows source indexes with a normal distribution of mean 2.0 and dispersion 0.2. When the SNR distribution in spiral arms is taken as the source distribution, we obtain the dashed line for sources with fixed injection index $s = 2.0$ and the dash-dotted line for source indexes with a normal distribution of mean 2.0 and dispersion 0.2.

hand, the locally observed spectra are strongly affected by solar modulation, for which we do not have reliable models, so that only over roughly one decade in energy does the local electron spectrum provide clear data. Figure 4 shows the data from direct electron measurements compared with the steady-state spectra of our model. The model spectra fit the data reasonably well in the relevant energy range, up to 30 GeV.

4.2. *The γ-Ray Emission*

As an example, we show in Figure 5 the spectra of the bremsstrahlung and inverse Compton emission in the direction of the inner Galaxy for the case of sources with injection indexes following a normal distribution of mean $s = 2.0$ and dispersion $\mu = 0.2$. This figure includes the results of our model, the observed spectrum, and a template of the π^0-decay spectrum (Dermer 1986). At around 5 GeV, the intensity from leptonic processes is higher than that from hadronic π^0 decay. Our model assumes that the power-law behavior of the electron injection spectra persists to $\sim$20 TeV. The high-energy γ-ray spectrum will rather directly reflect structure in the electron source spectra. If, for example, the true source spectrum deviates from a simple power law above 1 TeV, the inverse Compton spectrum would show corresponding features above 50 GeV.

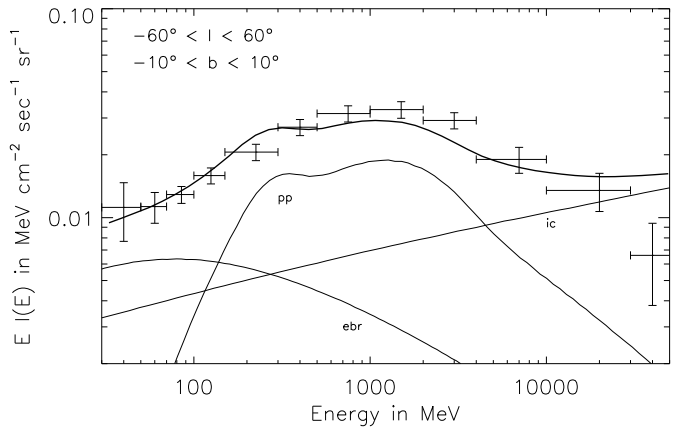

FIG. 5.—Gamma-ray intensity in the direction of the inner Galaxy. The data points are taken from Hunter et al. (1997). The error bars include an estimate for the systematic error of 8%, which accounts for the uncertainty in the energy-dependent correction of the spark chamber efficiency (Esposito et al. 1998). The data are compared with bremsstrahlung ("ebr") and Inverse Compton ("ic") spectra from our model, on the basis of sources with injection indexes following a normal distribution of mean 2.0 and dispersion 0.2 and the spatial distribution of SNRs in spiral arms. The π^0-component is a template and not a model.

When we consider the latitude distribution of the γ-ray intensity above 1 GeV, as shown in Figure 6, we find a high level of agreement. The fraction of the total diffuse intensity attributable to leptonic emission is almost constant between $b = 0°$ and $b = 10°$. It goes up from $\sim$6% in the Hunter et al. (1997) model to $\sim$10% in our model for an injection index of $s = 2.4$, to 30%–48% for an injection index of $s = 2.0$, enough to explain all the γ-ray excess.

We can compare the longitude distribution of the observed diffuse γ-ray emission above 1 GeV to that of the leptonic contribution in our model. This is done in Figure 7. It is obvious that the Galactocentric gradient of the leptonic γ-ray emission in our model is stronger than in the data. This is the case for all cosmic-ray propagation models that are based on the SNR distribution (Webber et al. 1992; Bloemen et al. 1993). While toward the inner Galaxy the fraction of the total diffuse intensity from leptonic emission is around 35%–52%, large enough to explain all the γ-ray excess, toward the outer Galaxy the leptonic contribution in our model accounts only for roughly two-thirds of the excess.

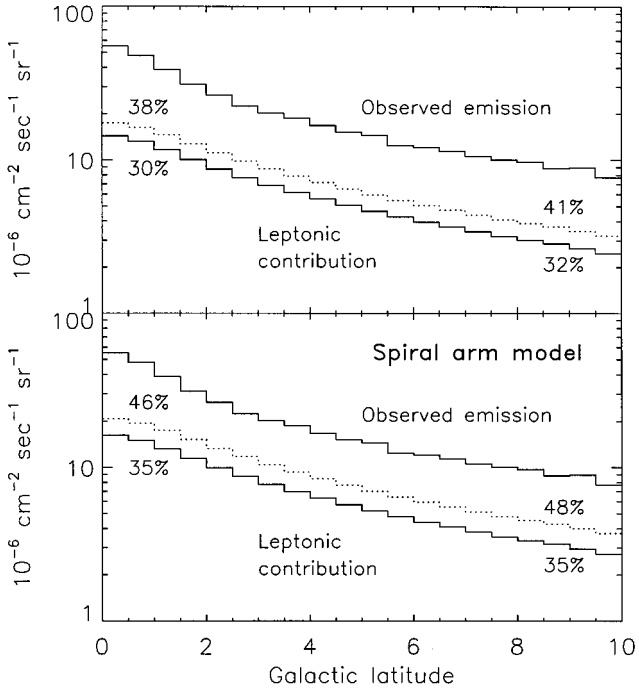

FIG. 6.—Latitude distribution of the γ-ray emission above 1 GeV compared with the model prediction for the leptonic contribution. The solid line shows the fixed injection index, and the dotted line shows a distribution of indexes with dispersion 0.2. The numbers give the percentage of the observed emission in certain directions that is due to leptonic processes. The top panel displays results for the pure SNR distribution as electron source distribution, while the bottom panel shows results for a source distribution of SNRs in spiral arms.

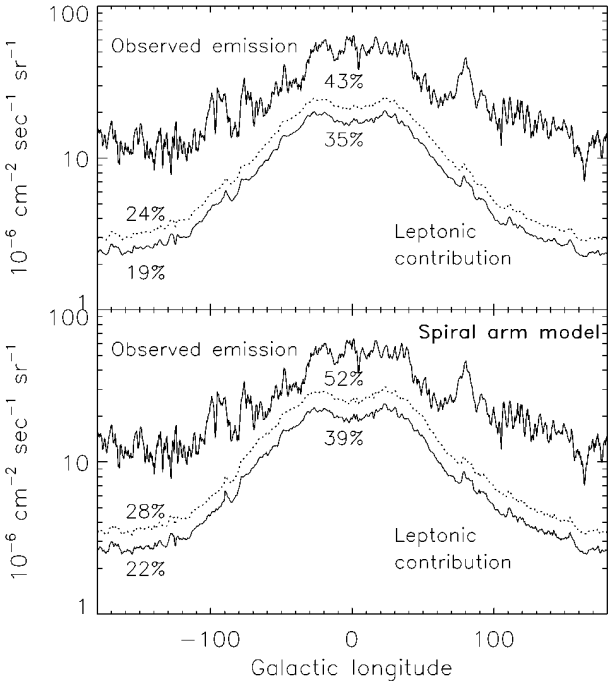

FIG. 7.—Longitude distribution of the γ-ray emission above 1 GeV. The upper solid line shows the observed distribution according to Hunter et al. (1997). The distribution of the leptonic emission in our model is shown for comparison, here for the SNR distribution as source distribution. The solid line shows a fixed injection index, and the dotted line shows a distribution of indexes with dispersion 0.2. Numbers on the plot give the percentage of the observed emission in certain directions that is due to leptonic processes. The top panel shows results for a pure SNR distribution, and the bottom panel shows results for the source distribution of SNRs in spiral arms.

The SNR distribution of Case & Bhattacharya (1996) is zero at Galactocentric radius $r = 0$, causing the double-peaked structure in the model intensity toward the inner Galaxy. Such a double-peaked structure is not visible in the data, so this effect may be the result of the specific choice of the mathematical function in the fit of the SNR distribution, rather than astrophysical reality. We can generally say that a flatter SNR distribution would beget a better harmony between the longitude distribution of observed emission and the model. Interestingly, one study of the SNR distribution that was not based on a specific form of the radial profile indicates very long radial scale lengths, up to 9 kpc (Li et al. 1991).

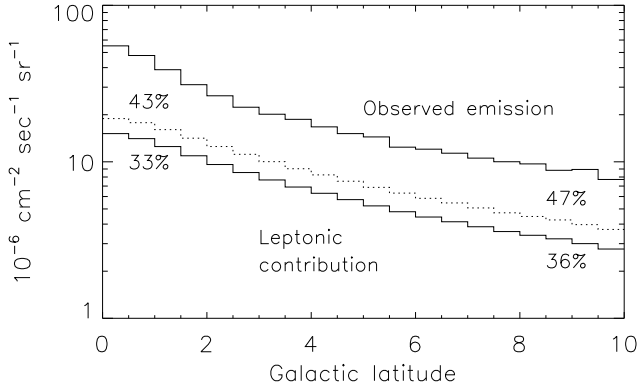

FIG. 8.—Latitude distribution of the γ-ray emission above 1 GeV, as in Fig. 6, except that here the flatter SNR distribution in spiral arms has been used. The indicated 33%–47% leptonic contribution is sufficient to account for all the excess.

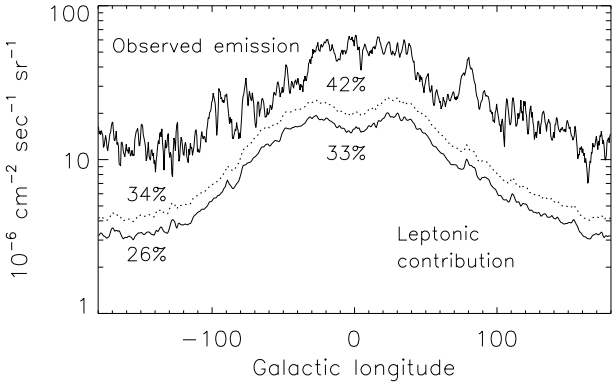

FIG. 9.—Longitude distribution of the γ-ray emission above 1 GeV, as in Fig. 7, except that here the flatter SNR distribution in spiral arms has been used. The overall gradient is well reproduced. The double-hump structure toward the inner Galaxy and the overprediction around $|l| \approx 45°$ indicate that the mathematical profile in the fit to the SNR distribution may be ill-defined.

We have therefore investigated the impact of the fit uncertainties in the SNR distribution. Within 1 σ in both parameters, the SNR distribution may be

$$f(r) = \left(\frac{r}{r_\odot}\right)^{1.91} \exp\left(-2.96\,\frac{r - r_\odot}{r_\odot}\right). \qquad (21)$$

Here we show the results for the spiral-arm model only. For similar local electron spectra, the leptonic contribution to the diffuse Galactic γ-ray emission above 1 GeV can be 33%–47%, while the center/anticenter contrast in the model agrees with the observed one to better than 25%. As can be seen in Figure 8, the latitude distribution of the leptonic contribution varies little. The longitude distribution of the leptonic contribution in Figure 9 shows that the overall gradient is reasonably well reproduced, but the double-hump structure toward the inner Galaxy remains, as does a general overprediction around $|l| \approx 45°$. However, this double-hump structure is a consequence of the mathematical function chosen to fit the SNR distribution, not a characteristic of the SNR distribution itself.

4.3. *The Synchrotron Emission*

A further constraint on our model is the synchrotron flux toward the north Galactic pole (NGP). Available data at

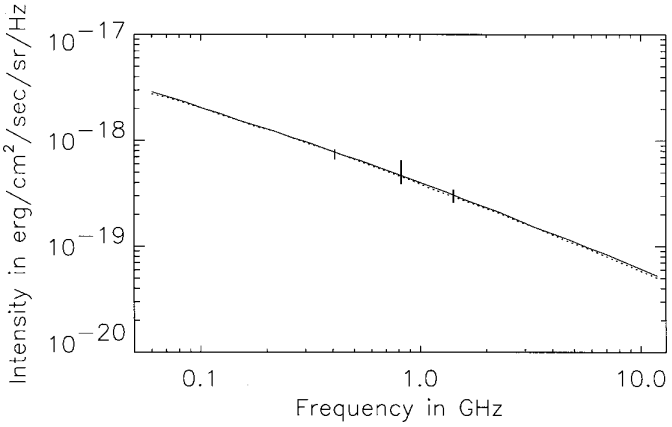

FIG. 10.—Synchrotron intensity in the direction of the north Galactic pole. The error bars indicate data from surveys with reasonable zero-level calibration. The solid line shows a model spectrum based on the pure SNR source distribution, while the dotted line shows a spectrum for the SNRs distributed in spiral arms.

408 MHz (Haslam et al. 1982), 820 MHz (Berkhuijsen 1972), and 1420 MHz (Reich & Reich 1986) can be corrected for zero-level uncertainties, contributions from the microwave background and unresolved extragalactic sources (Reich & Reich 1988), and contributions from the Coma cluster (Schlickeiser, Sievers, & Thiemann 1987). Here we do not use data at frequencies below 100 MHz, which we expect to be affected by free-free absorption. In Figure 10 we compare the synchrotron intensity predicted by our model with the data in the direction of the NGP. It can be seen that for a total magnetic field strength of 10 μG, there is good agreement.

In our model, the FWHM of the z-distribution of synchrotron emission at 1420 MHz is ~ 1.1 kpc, which is the value typically found for edge-on galaxies (Hummel 1991).

5. SUMMARY AND DISCUSSION

In this paper we have investigated whether cosmic-ray electrons could be responsible for the recently observed high intensity of diffuse Galactic γ-ray emission above 1 GeV. Models based on the locally observed cosmic-ray spectra underpredict the observed intensity by nearly 40% (Hunter et al. 1997). One feature of these models is the relatively soft electron injection spectral index of $s = 2.4$ (Skibo 1993) that is required to account for the local electron spectrum above 50 GeV.

The recent detection of nonthermal X-ray synchrotron radiation from the four supernova remnants SN 1006 (Koyama et al. 1995), RX J1713.7$-$3946 (Koyama et al. 1997), IC 443 (Keohane et al. 1997), and Cas A (Allen et al. 1997) supports the hypothesis that Galactic cosmic-ray electrons are accelerated predominantly in SNRs. We have shown in this paper that if this is indeed the case, the local electron spectra above 30 GeV are variable on timescales of a few hundred thousand yr. This variability stems from the Poisson fluctuations in the number of SNRs in the solar vicinity within a certain time period. While the electron spectra below 10 GeV are stable, the level of fluctuation increases with electron energy, and above 100 GeV the local electron flux is more or less unpredictable.

With that time variability in mind, we have seen that an electron injection index of $s = 2.0$ is consistent with the data of the direct particle measurements if SNRs are the dominant source of cosmic-ray electrons. In fact, both the radio spectra of individual SNRs (Green 1995) and the hard spectrum of the inverse Compton emission at high latitudes (Chen, Dwyer, & Kaaret 1996) would better harmonize with an injection index of $s = 2.0$, rather than $s = 2.4$.

We have presented a three-dimensional steady-state diffusion model for cosmic-ray electrons, based on propagation parameters that have been derived from similar models for cosmic-ray nucleons. While remaining entirely consistent with the local electron flux up to ~ 30 GeV energy and with the radio synchrotron spectrum toward the north Galactic pole, the leptonic contribution to the diffuse Galactic γ-ray emission above 1 GeV in the Galactic plane increases from $\sim 6\%$ in the model of Hunter et al. (1997) to $\sim 10\%$ in our model for an injection index of $s = 2.4$, to 30%–48% for an injection index of $s = 2.0$, depending on the assumed spatial distribution of SNRs and on whether some dispersion of injection spectral indexes is allowed. An electron injection index of $s = 2.0$ can therefore explain the bulk of the observed γ-ray excess over the predictions of the Hunter et al. model.

While the latitude distribution of the leptonic γ-ray emission is fully consistent with that of the observed emission, we find that the longitude distribution deviates from the observed one. The contrast between the Galactic center and the anticenter is stronger in our model than in the data. A similar effect can be found in all cosmic-ray propagation models that are based on the SNR distribution (Webber et al. 1992; Bloemen et al. 1993). Note that in the Hunter et al. (1997) model, only the emissivity spectrum is taken according to a propagation calculation (Skibo 1993), while the spatial distribution of the emissivity is scaled according to the distribution of thermal gas.

We have seen that the fitted uncertainties in the SNR distribution of Case & Batthacharya (1996) allow us to use a flatter profile, which leads to a better agreement between the model and the data in the longitude distribution (see Fig. 9). Thus, the gradient problem may be simply the result of an inappropriate choice of radial SNR distribution or the lack of error propagation, respectively. This flatter profile would also harmonize better with the results of Li et al. (1991), who found very large radial scale lengths of up to 9 kpc for the Galactic distribution of SNRs. Other possible sources of systematic errors are discussed below.

This gradient problem is unlikely to be caused by additional thermal matter. Very cold (3° K) molecular gas has recently been discussed as a candidate for baryonic dark matter (Pfenniger, Combes, & Martinet 1994). If organized in small clumps (Pfenniger & Combes 1994), the probability of finding absorption features in the spectra of bright background objects would be small, and the clumps could easily evade detection (for a review see Combes & Pfenniger 1997). However, the thermal gas mainly affects the bremsstrahlung and only indirectly the inverse Compton emission, which dominates above 1 GeV γ-ray energy, and thus has little influence on the gradient of the total leptonic γ-ray emission above 1 GeV.

If our model for the interstellar radiation field were wrong, then it would have only a limited influence on the gradient, since the Galaxy acts as a fractional calorimeter at high electron energies (Pohl 1994), channeling the electron source power directly into synchrotron and inverse Compton emission with a ratio corresponding to the ratio of the energy densities in the magnetic field and the photon field. Any radial variation of the magnetic field strength will be directly reflected in the center/anticenter contrast of the synchrotron intensity, so that the radio surveys would constrain the parameter space here.

It is our personal view that the uncertainties in the radial distribution of SNRs are large enough that the overly strong gradient in our model may simply be the result of an inappropriate choice of SNR distribution. The artificial double-peaked structure toward the inner Galaxy is an example of systematic effects arising from possibly ill-defined fits to the SNR distribution.

Our findings indicate a potential problem in the determination of the extragalactic γ-ray background (Sreekumar et al. 1998). The standard method uses a linear regression analysis of observed intensities and model predictions (with the model of Hunter et al. 1997) to extrapolate to zero Galactic intensity. If at higher γ-ray energies the inverse Compton emission is indeed much stronger than assumed by Hunter et al. (1997), then a large fraction of it will be attributed to the extragalactic γ-ray emission. Our steady-state model predicts an intensity of high-latitude inverse

Compton emission above 1 GeV at a level of $\sim 40\%$ of the extragalactic background intensity, while Hunter et al. (1997) assume much smaller values. The intensity difference between the inner Galaxy and the outer Galaxy at medium latitudes (40°–50°) would be around 10% of the extragalactic background intensity, depending on the choice of model for the electron source distribution (SNR distribution). On the other hand, if we are indeed living in a region of temporarily low flux of high-energy electrons, we would also expect the intensity of inverse Compton emission toward the Galactic poles to be less that the steady-state value, making the true level of Galactic γ-ray intensity at high latitudes is difficult to assess.

The spectrum of inverse Compton emission, $s \simeq 1.85$ in our model, is somewhat harder than the $s \simeq 2.1$ of the extragalactic background. It has been noted before that the average γ-ray spectrum of the identified active galactic nuclei (AGNs) is softer than that of the background (Pohl et al. 1997a), which indicates a problem with the idea that the background is mainly due to unresolved AGNs. Now, since the presently determined background spectrum may be substantially contaminated by hard inverse Compton emission, the true background spectrum may be softer than $s = 2.1$, which would probably relieve the spectral discrepancy with the average spectrum of resolved AGNs (Pohl et al. 1997a). In any case, the systematic uncertainty in the spectral index of the extragalactic γ-ray background emission is much higher than the statistical uncertainty.

In a forthcoming paper we will discuss the distribution of synchrotron emission in more detail. We will also use a truly three-dimensional calculation of the interstellar photon fields based on *COBE*/FIRAS data. Finally, we will discuss cosmic-ray nucleons in parallel with electrons in order to derive the propagation parameters self-consistently.

The EGRET Team gratefully acknowledges support from the following: Bundesministerium für Bildung, Wissenschaft, Forschung und Technologie (BMBF), Grant 50 QV 9095 (MPE); NASA Cooperative Agreement NCC 5-93 (HSC); NASA Cooperative Agreement NCC 5-95 (SU); NASA Contract NAS 5-96051 (NGC); and NASA Contract NAS 5-32490 (USRA).

REFERENCES

Allen, G. E., et al. 1997, ApJ, 487, L97
Arimoto, N., Sofue, Y., & Tsujimoto, T. 1996, PASJ, 48, 275
Barwick, S. W., et al. 1997, ApJ, 482, L191
Berkey, G. B., & Shen, C. S. 1969, Phys. Rev., 188, 1994
Berkhuijsen, E. M. 1972, A&AS, 5, 263
Bertsch, D. L., et al. 1993, ApJ, 416, 587
Blandford, R., & Eichler, D. 1987, Phys. Rep., 154, 1
Bloemen, H. 1989, ARA&A, 27, 469
Bloemen, H., et al. 1993, A&A, 267, 372
Bonino, G. 1996, Nuovo Cimento, 19C, 865
Brecher, K., & Burbidge, G. R. 1972, ApJ, 174, 253
Buckley, J. H., et al. 1998, A&A, 329, 639
Burton, W. B. 1985, A&AS, 62, 365
———. 1976, ARA&A, 14, 275
Burton, W. B., & Liszt, H. S. 1983, A&AS, 52, 63
Cappelaro, E., et al. 1997, A&A, 321, 431
Case, G., & Bhattacharya, D. 1996, A&AS, 120, C437
Chen, A., Dwyer, J., & Kaaret, P. 1996, ApJ, 463, 169
Cleary, M. N., Heiles, C., & Haslam, C. G. T. 1979, A&AS, 36, 95
Clemens, D. P. 1985, ApJ, 295, 422
Combes, F., & Pfenniger, D. 1997, A&A, 327, 453
Cowsik, R., & Lee, M. A. 1979, ApJ, 228, 297
Dame, T. M., et al. 1987, ApJ, 322, 706
Dermer, C. D. 1986, A&A, 157, 223
Digel, S. W., et al. 1996, ApJ, 463, 609
Digel, S. W., Hunter, S. D., & Mukherjee, R. 1995, ApJ, 441, 270
Dogiel, V. A., & Uryson, A. V. 1988, A&A, 197, 335
Drury, L. O'C., Aharonian, F. A., & Völk, H. J. 1994, A&A, 287, 959
Esposito, J. A., et al. 1998, ApJ, submitted
Fazio, G. G., Stecker, F. W., & Wright, J. P. 1966, ApJ, 144, 611
Ferrando, P., et al. 1996, A&A, 316, 528
Fichtel, C. E., et al. 1975, ApJ, 198, 163
Georgelin, Y. M., & Georgelin, Y. P. 1976, A&A, 49, 57
Ginzburg, V. L., & Syrovatskii, S. I. 1964, The Origin of Cosmic Rays (Oxford: Pergamon)
Gleeson, L. J., & Axford, W. I. 1968, ApJ, 154, 1011
Golden, R. L., et al. 1994, ApJ, 436, 769
———. 1984, ApJ, 287, 622
Green, D. A. 1995, A Catalogue of Galactic SNR (Cambridge: Mullard RAO)
Hammersley, P. L., et al. 1995, MNRAS, 273, 206
Haslam, C. G. T., et al. 1982, A&AS, 47, 1
Heiles, C., & Habing, H. J. 1974, A&AS, 14, 557
Hummel, E. 1991, in IAU Symp. 144, The Interstellar Disk-Halo Connection in Galaxies, ed. H. Bloemen (Dordrecht: Kluwer), 257
Hunter, S. D., et al. 1997, ApJ, 481, 205
———. 1994, ApJ, 436, 216
Keohane, J. W., et al. 1997, ApJ, 484, 350
Kerr, F. J., et al. 1986, A&AS, 66, 373
Kocharov, G. E. 1996, Nuovo Cimento, 19C, 883
Kodaira, K. 1974, PASJ, 26, 255
Koyama, K., et al. 1997, PASJ, 49, L7
———. 1995, Nature, 378, 255
Kraushaar, W., et al. 1972, ApJ, 177, 341
Lerche, I., & Schlickeiser, R. 1981, ApJS, 47, 33
———. 1982, MNRAS, 201, 1041
———. 1982, A&A, 107, 148
Lessard, R. W., et al. 1995, 24th ICRC, 2, 475
Li, Z., Wheeler, J. C., Bash, F. N., & Jefferys, W. H. 1991, ApJ, 378, 93
Mayer-Hasselwander, H., et al. 1982, A&A, 105, 164
McHargue, L. R., Damon, P. E., & Donahue, D. J. 1995, Geophys. Res. Lett., 22, 659
McLaughlin, M. A., et al. 1996, ApJ, 473, 763
Merck, M., et al. 1996, A&AS, 120, C465
Mori, M. 1997, ApJ, 478, 225
Pfenniger, D., & Combes, F. 1994, A&A, 285, 94
Pfenniger, D., Combes, F., & Martinet, L. 1994, A&A, 285, 79
Pohl, M. 1996, A&A, 307, L57
———. 1994, A&A, 287, 453
Pohl, M., Hartman, R. C., Jones, B. B., & Sreekumar, P. 1997a, A&A, 326, 51
Pohl, M., Kanbach, G., Hunter, S. D., & Jones, B. B. 1997b, ApJ, 491, 159
Pohl, M., & Schlickeiser, R. 1990, A&A, 234, 147
Porter, T. A., & Protheroe, R. J. 1997, J. Phys. G, 23, 1765
Reich, P., & Reich, W. 1986, A&AS, 63, 205
———. 1988, A&AS, 74, 7
Schlickeiser, R. 1982, A&A, 106, L5
Schlickeiser, R., Pohl, M., Ramaty, R., & Skibo, J. G. 1997, in AIP Conf. Proc. 410, Proc. 4th Compton Symp., ed. C. D. Dermer, M. S. Strickman, & J. D. Kurfess (New York: AIP), 449
Schlickeiser, R., Sievers, A., & Thiemann, H. 1987, A&A, 182, 21
Skibo, J. G. 1993, Ph.D. thesis, Univ. Maryland
Sodroski, T. J., et al. 1995, ApJ, 452, 262
Sonnett, C. P., et al. 1987, Nature, 330, 458
Sreekumar, P., et al. 1993, Phys. Rev. Lett., 70, 127
———. 1998, ApJ, 494, 523
Stecker, F. W., & Jones, F. C. 1977, ApJ, 217, 843
Strong, A. W. 1995, Space Sci. Rev., 76, 205
Strong, A. W., & Mattox, J. R. 1996, A&A, 308, L21
Strong, A. W., et al. 1988, A&A, 207, 1
Taira, T., et al. 1993, Proc. 23d Int. Cosmic-Ray Conf. (Calgary), 2, 128
Tang, K. K. 1984, ApJ, 278, 881
Tanimori, T., et al. 1997, IAU Circ. No. 6706
Taylor, J. H., & Cordes, J. M. 1993, ApJ, 411, 674
Vallée, J. P. 1995, ApJ, 454, 119
Weaver, H. F., & Williams, D. R. W. 1973, A&AS, 8, 1
Webber, W. R., Lee, M. A., & Gupta, M. 1992, ApJ, 390, 96
Webster, A. S. 1970, Astrophys. Lett., 5, 189
Youssefi, G., & Strong, A. W. 1991, Proc. 22d Int. Cosmic-Ray Conf. (Dublin), 1, 129